Ministry of Energy of the Republic of Kazakhstan
Institute of Nuclear Physics

INTERNATIONAL SCHOOL
“Introduction to High-Energy Physics, Accelerator Technology and Nuclear Medicine”

Quasiperiodic oscillations from low mass X-ray binary systems

Kuantay Boshkayev

in collaboration with

M. Muccino and H.Quevedo

Al-Farabi Kazakh National University, Almaty, Kazakhstan

ALMATY, KAZAKHSTAN
October 09-13, 2023

Motivation

Investigation of the motion of test particles in the field of rotating and deformed objects are relevant to several astrophysical phenomena:

- in particular to the observed high frequency, kilohertz Quasi Periodic Oscillations (kHz QPOs) in the X-ray luminosity from black hole and neutron star sources;
- it is believed that kHz QPO data may be used to test the strong field regime of Einstein's general relativity, and the physics of super-dense matter of which neutron stars are made of.

External Hartle-Thorne Solution

$$ds^2 = -\left(1 - \frac{2M}{r}\right)\left[1 + 2k_1 P_2(\cos\theta) + 2\left(1 - \frac{2M}{r}\right)^{-1}\frac{J^2}{r^4}(2\cos^2\theta - 1)\right]dt^2$$

$$+\left(1 - \frac{2M}{r}\right)^{-1}\left[1 - 2k_2 P_2(\cos\theta) - 2\left(1 - \frac{2M}{r}\right)^{-1}\frac{J^2}{r^4}\right]dr^2$$

$$+r^2[1 - 2k_3 P_2(\cos\theta)](d\theta^2 + \sin^2\theta d\phi^2) - 4\frac{J}{r}\sin^2\theta dt d\phi$$

$$k_1 = \frac{J^2}{Mr^3}\left(1 + \frac{M}{r}\right) - \frac{5}{8}\frac{Q - J^2/M}{M^3}Q_2^2\left(\frac{r}{M} - 1\right), \qquad k_2 = k_1 - \frac{6J^2}{r^4},$$

$$k_3 = k_1 + \frac{J^2}{r^4} - \frac{5}{4}\frac{Q - J^2/M}{M^2 r}\left(1 - \frac{2M}{r}\right)^{-1/2}Q_2^1\left(\frac{r}{M} - 1\right), \qquad P_2(x) = \frac{1}{2}(3x^2 - 1),$$

$$Q_2^1(x) = (x^2 - 1)^{1/2}\left[\frac{3x}{2}\ln\frac{x+1}{x-1} - \frac{3x^2 - 2}{x^2 - 1}\right], \qquad Q_2^2(x) = (x^2 - 1)\left[\frac{3}{2}\ln\frac{x+1}{x-1} - \frac{3x^3 - 5x}{(x^2 - 1)^2}\right].$$

- *Hartle, J. B., ApJ 150, 1005 (1967)*
- *Hartle, J. B. & Thorne, K. S., ApJ, 153, 807 (1968)*

Limiting cases

- Q=0, J=0, SCHW;
- Q=0, J≠0, neglecting terms ~ J^2, LT;
- Q≠0, J≠0, HT

or Kerr solution in the Boyer-Lindquist coordinates using the following substitution and coordinate transformations:

$$J = -Ma, \quad Q = J^2/M,$$

and

$$\begin{aligned} t &= t\,, \\ r &= R + \frac{a^2}{2R}\left[\left(1+\frac{2M}{R}\right)\left(1-\frac{M}{R}\right) - \cos^2\Theta\left(1-\frac{2M}{R}\right)\left(1+\frac{3M}{R}\right)\right], \\ \theta &= \Theta + \frac{a^2}{2R^2}\left(1+\frac{2M}{R}\right)\sin\Theta\cos\Theta\,, \\ \phi &= \phi. \end{aligned}$$

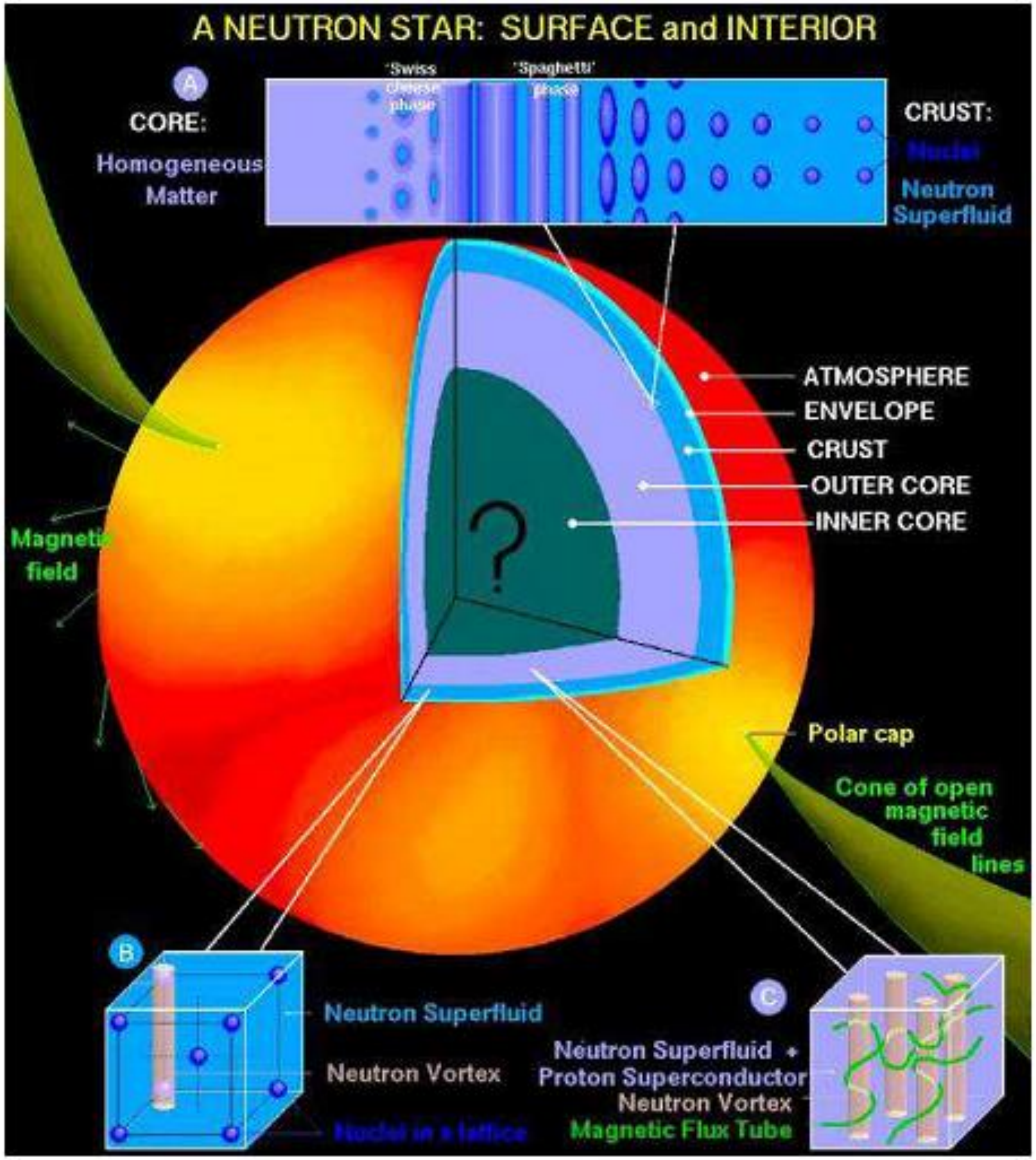

Figure 1 - Current observations of neutron star masses suggest the existence of stars with a mass of order 2 solar masses. Such stars require a **stiff equation of state** for the neutron matter that makes up most of the star to be able to balance the attraction of gravity and rules out the presence of **exotic forms of matter (pion-kaon condensates, quark matter or core solids)** in the core of any neutron star because at any mass its central density is less than the transition densities for these exotic phases.

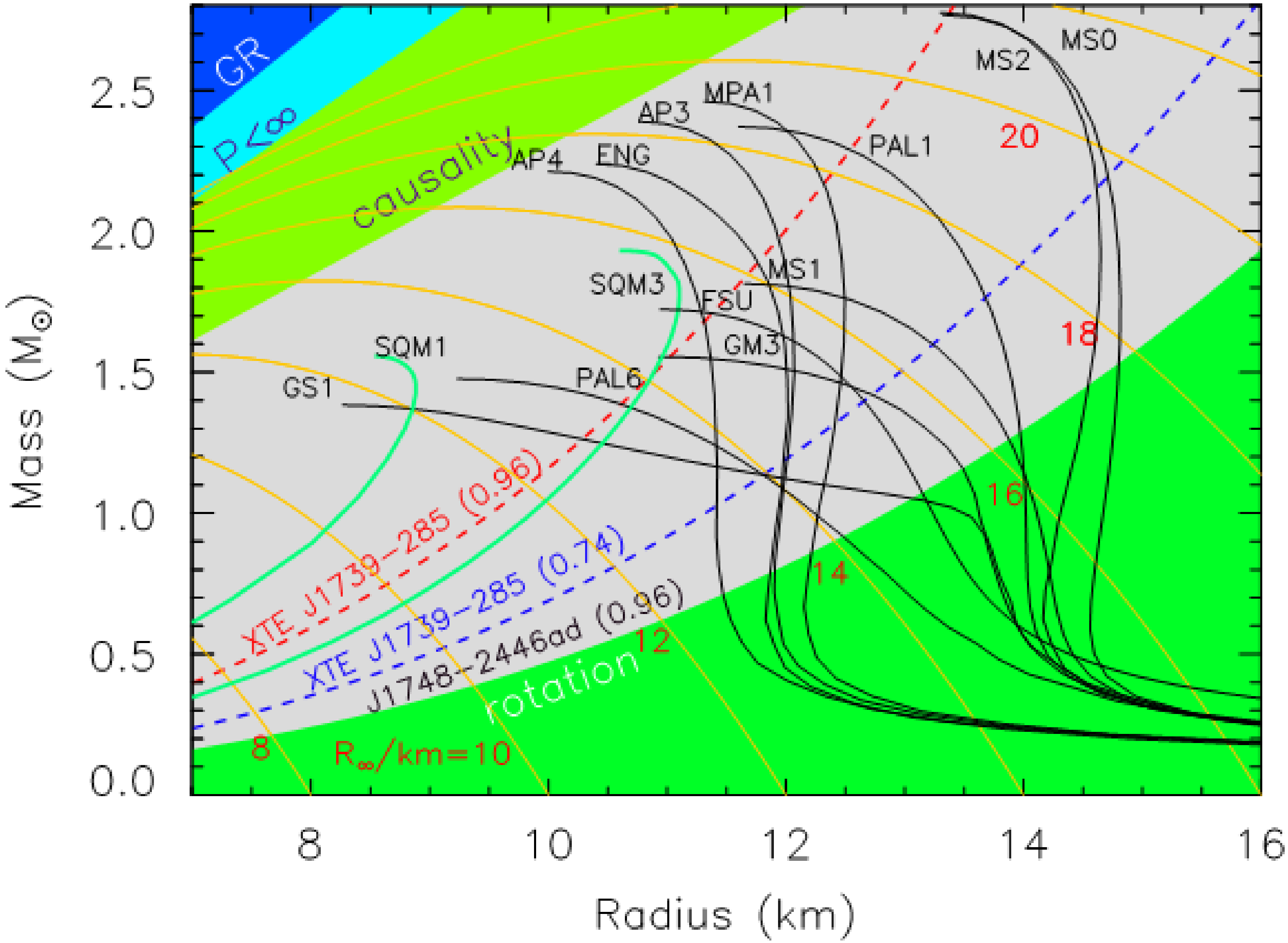

Figure 2 – Mass-Radius relations of Neutron Stars.
J.M. Lattimer, M. Prakash / Physics Reports 442 (2007) 109–165

Neutron Star Model

Belvedere, R.; Pugliese, D.; Rueda, J.A.; Ruffini, R; Xue, Sh.
“Neutron star equilibrium configurations within a fully relativistic theory with strong, weak, electromagnetic, and gravitational interactions”
Nuclear Physics A, Volume 883, p. 1-24. 2012

Belvedere, R.; Boshkayev, K.; Rueda, Jorge A.; Ruffini, R.
“Uniformly rotating neutron stars in the global and local charge neutrality cases”
Nuclear Physics A, Volume 921, p. 33-59. 2014

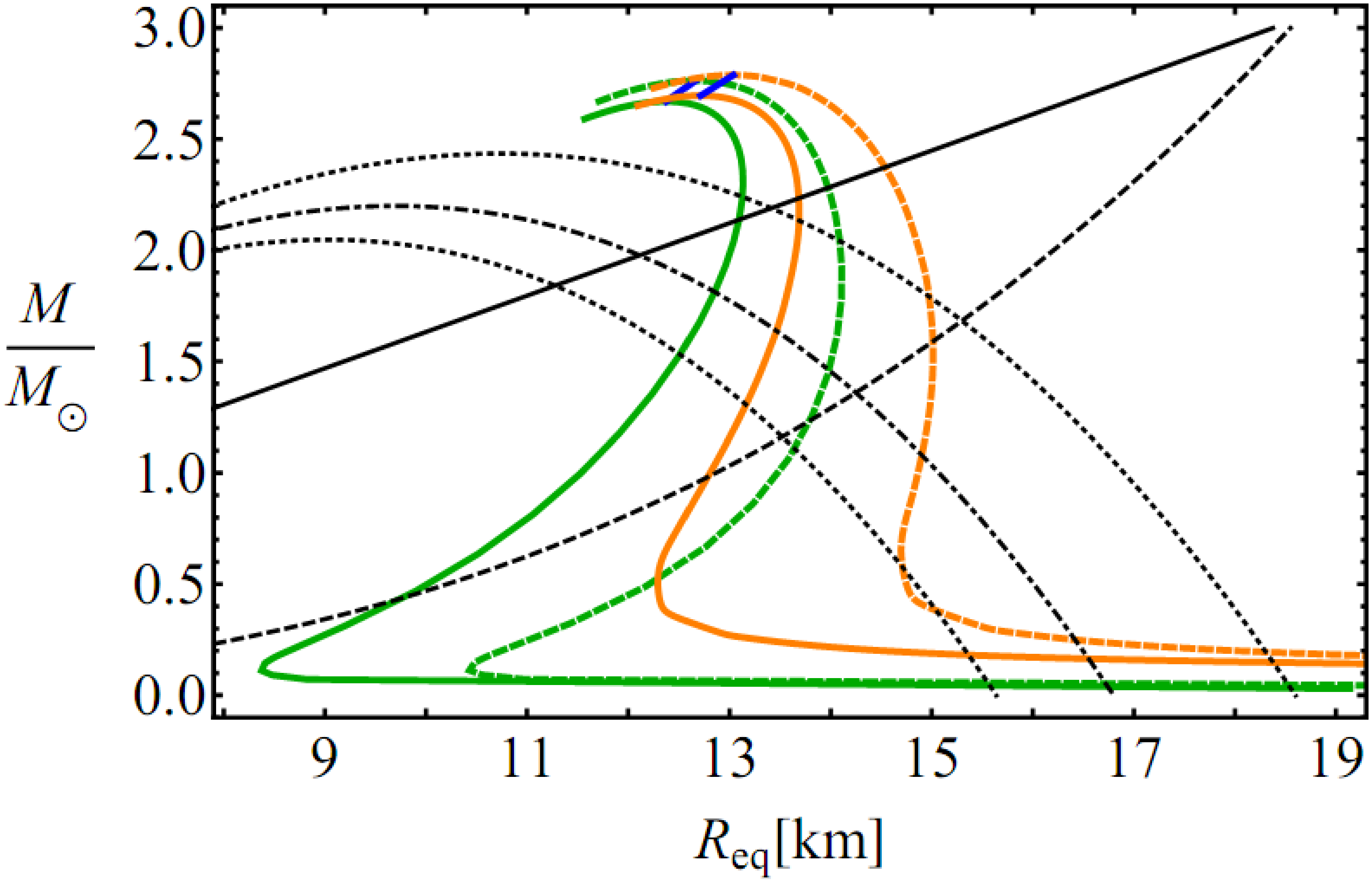

Figure 3 – Mass-Radius relations for Neutron Stars

Belvedere et. al. Nuclear Physics A, Volume 883, p. 1-24. (2012)
Belvedere et. al. Nuclear Physics A, Volume 921, p. 33-59. (2014)

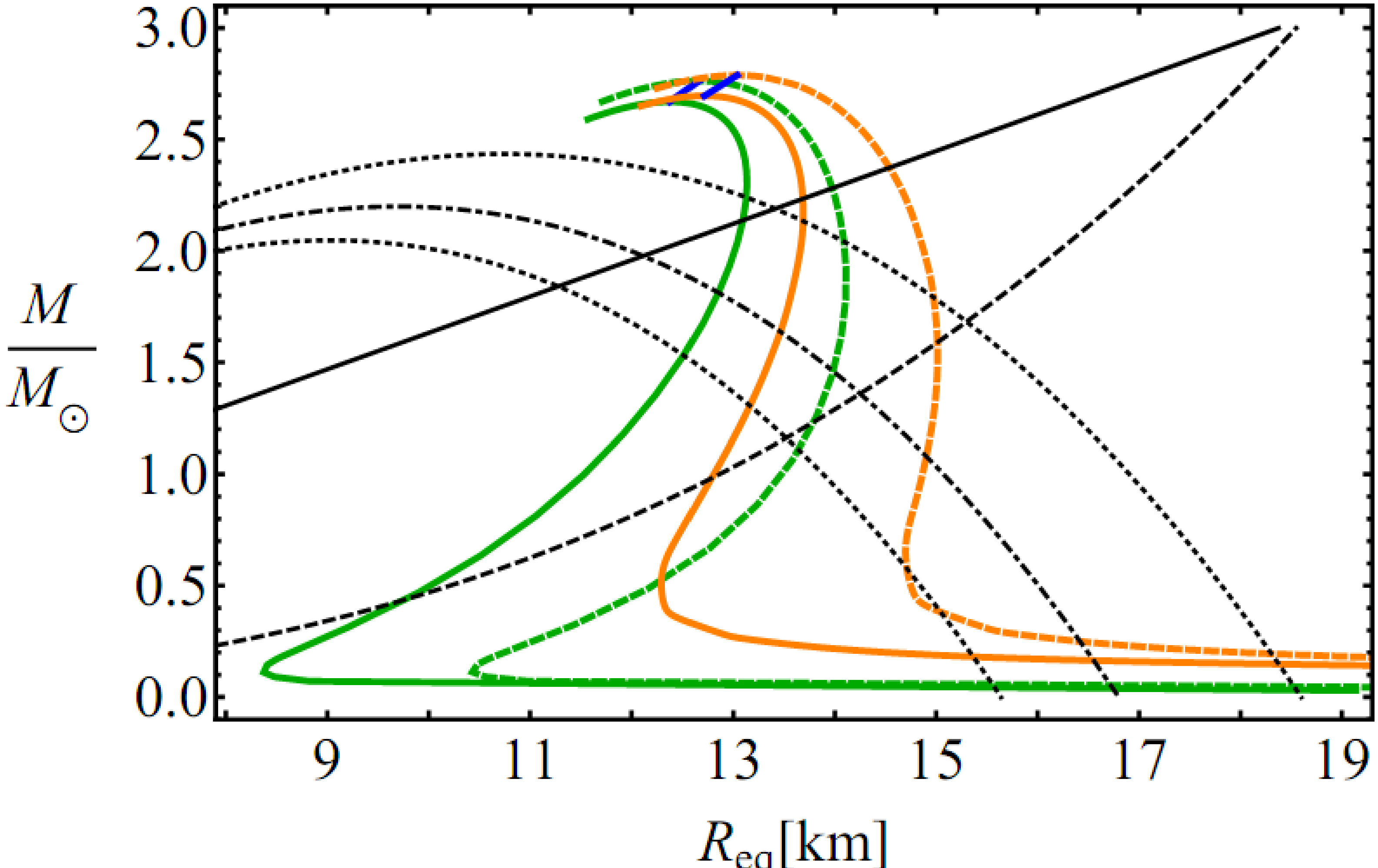

Constraints on the mass-radius relation given by J. E. Trumper in and the theoretical mass-radius in our work **the solid line is the upper limit of the surface gravity of XTE J1814-338**, **the dotted-dashed curve corresponds to the lower limit to the radius of RX J1856-3754, the dashed line is the constraint imposed by the fastest spinning pulsar PSR J1748-2246ad, and the dotted curves are the 90% confidence level contours of constant R_∞ of the neutron star in the low-mass X-ray binary X7**. Any mass-radius relation should pass through the area delimited by the solid, the dashed and the dotted lines and, in addition, it must have a maximum mass larger than the mass of PSR J1614-2230, $M = 1.97 \pm 0.04 M_{\odot}$.

QPOs

In X-ray astronomy, **quasi-periodic oscillation** (**QPO**) is the manner in which the X-ray light from an astronomical object flickers about certain frequencies. In these situations, the X-rays are emitted near the inner edge of an accretion disk in which gas swirls onto a compact object such as a white dwarf, neutron star, or black hole.

QPOs were first identified in white dwarf systems and then in neutron star systems.

van der Klis et al. 1985, Nature, 316, 225
Middleditch and Priedhorsky 1986, Astrophysical Journal 306, 230

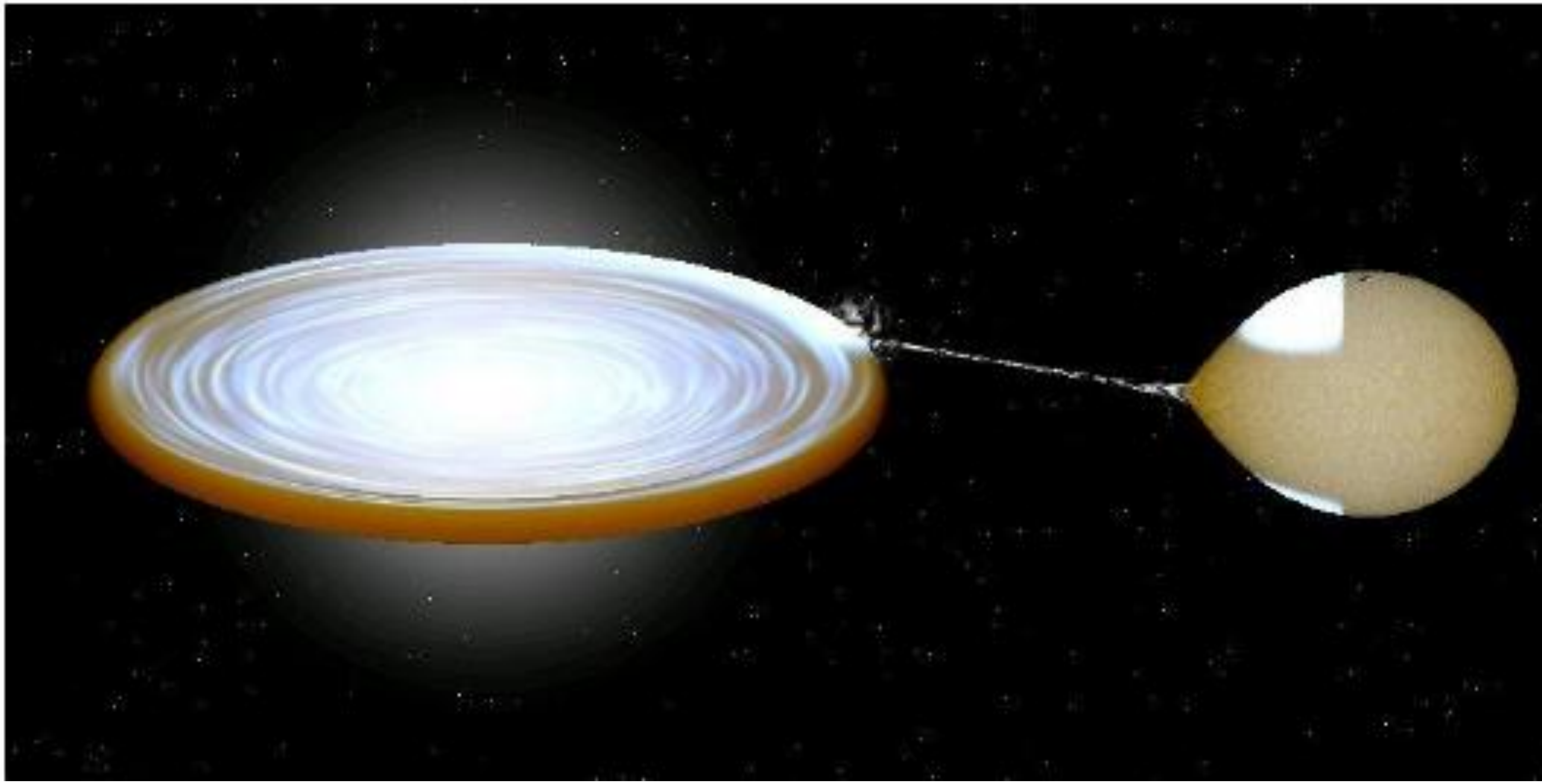

Figure 4 - Artist view of a LMXB system (http.//astro.virginia.edu)

In the context of X-ray binary systems, which often involve compact objects like neutron stars and black holes, QPOs are observed in the X-ray emissions. The frequency of QPOs in these systems typically falls within the range of approximately 0.1 Hz (hertz) to several hundred hertz. The exact frequency range can vary from one binary system to another and may depend on the properties of the compact object and the accretion disk.

Origin of QPOs: Quasiperiodic oscillations, on the other hand, originate from different processes within the X-ray binary system. QPOs are often associated with variations in the X-ray emission and are thought to be linked to dynamic and complex interactions in the system, including the accretion disk and the compact object.

Modulation Frequency: The frequency of QPOs represents the characteristic timescales of the physical processes driving the variations in the X-ray emissions. These timescales can be significantly longer than the timescales associated with the production of X-rays. As a result, QPO frequencies are typically much lower, falling in the range of about 0.1 Hz to several hundred hertz.

The Relativistic Precession Model (RPM)

The RPM has been proposed in a series of papers by Stella and Vietri. *It explains the kHz QPOs as a direct manifestation of modes of relativistic epicyclic motion of blobs arising at various radii r in the inner parts of the accretion disk. The model identifies the lower and upper kHz QPOs with the periastron precession* f_{per} *and Keplerian* f_K *frequency.*

$$f_L = f_{per} = f_\phi - f_r \qquad\qquad f_U = f_\phi = f_K$$

$$\Delta f = f_U - f_L = f_r$$

Stella, L., Vietri, M., 1999, Phys. Rev. Lett. , 82, 17.

Let us consider a generic stationary, axisymmetric, and asymptotically flat spacetime. We write the line element as

$$ds^2 = g_{tt}dt^2 + g_{rr}dr^2 + g_{\theta\theta}d\theta^2 + 2g_{t\varphi}dt d\varphi + g_{\varphi\varphi}d\varphi^2.$$

The metric coefficients are independent of the t and φ coordinates, leading to the existence of the conserved specific energy at infinity, E, and the conserved z-component of the specific angular momentum at infinity, L_z. The t- and φ-component of the 4-velocity of a test-particle can thus be written as

$$\dot{t} = \frac{E g_{\varphi\varphi} + L_z g_{t\varphi}}{g_{t\varphi}^2 - g_{tt}g_{\varphi\varphi}}. \qquad \dot{\varphi} = -\frac{E g_{t\varphi} + L_z g_{tt}}{g_{t\varphi}^2 - g_{tt}g_{\varphi\varphi}}. \qquad (1)$$

From the conservation of the rest-mass, $g_{\mu\nu}\dot{x}^{\mu}\dot{x}^{\nu} = -1$, we have

$$g_{rr}\dot{r}^2 + g_{\theta\theta}\dot{\theta}^2 = V_{\rm eff}(r, \theta, E, L_z), \tag{2}$$

where the effective potential $V_{\rm eff}$ is

$$V_{\rm eff} = \frac{E^2 g_{\varphi\varphi} + 2EL_z g_{t\varphi} + L_z^2 g_{tt}}{g_{t\varphi}^2 - g_{tt}g_{\varphi\varphi}} - 1. \tag{3}$$

Circular orbits in the equatorial plane have $\dot{r} = \dot{\theta} = \ddot{r} = 0$. We write the geodesic equations as

$$\frac{\mathrm{d}}{\mathrm{d}\lambda}\left(g_{\mu\nu}\dot{x}^{\nu}\right) = \frac{1}{2}\left(\partial_{\mu}g_{\nu\rho}\right)\dot{x}^{\nu}\dot{x}^{\rho}, \tag{4}$$

and we consider the radial component (namely $\mu = r$)

$$(\partial_r g_{tt})\,\dot{t}^2 + 2(\partial_r g_{t\varphi})\,\dot{t}\dot{\varphi} + (\partial_r g_{\varphi\varphi})\,\dot{\varphi}^2 = 0. \tag{5}$$

From eq. (5) we obtain the orbital angular velocity $\Omega_\varphi = \dot{\varphi}/\dot{t}$

$$\Omega_\varphi = \frac{-\partial_r g_{t\varphi} \pm \sqrt{(\partial_r g_{t\varphi})^2 - (\partial_r g_{tt})(\partial_r g_{\varphi\varphi})}}{\partial_r g_{\varphi\varphi}}, \qquad (6)$$

where the sign is + ($-$) for corotating (counter-rotating) orbits. The orbital frequency is thus $\nu_\varphi = \Omega_\varphi / 2\pi$

From $g_{\mu\nu}\dot{x}^\mu \dot{x}^\nu = -1$ with $\dot{r} = \dot{\theta} = 0$ we have

$$\dot{t} = \frac{1}{\sqrt{-g_{tt} - 2g_{t\varphi}\Omega_\varphi - g_{\varphi\varphi}\Omega_\varphi^2}}. \qquad (7)$$

The radial and vertical epicyclic frequencies can be obtained by studying small perturbations around circular equatorial orbits. If δ_r and δ_θ are the small displacements around the mean orbit (*i.e.*, $r = r_0 + \delta_r$ and $\theta = \pi/2 + \delta_\theta$), they are governed by the following differential equations:

$$\frac{d^2\delta_r}{dt^2} + \Omega_r^2\delta_r = 0, \quad \frac{d^2\delta_\theta}{dt^2} + \Omega_\theta^2\delta_\theta = 0, \qquad (10)$$

where

$$\Omega_r^2 = -\frac{1}{2g_{rr}\dot{t}^2}\frac{\partial^2 V_{\rm eff}}{\partial r^2}, \quad \Omega_\theta^2 = -\frac{1}{2g_{\theta\theta}\dot{t}^2}\frac{\partial^2 V_{\rm eff}}{\partial \theta^2}. \qquad (11)$$

The radial epicyclic frequency is $\nu_r = \Omega_r/2\pi$. The vertical epicyclic frequency is $\nu_\theta = \Omega_\theta/2\pi$.

$$f_L = f_{per} = f_\phi - f_r \qquad f_U = f_\phi = f_K$$

$$\Delta f = f_U - f_L = f_r$$

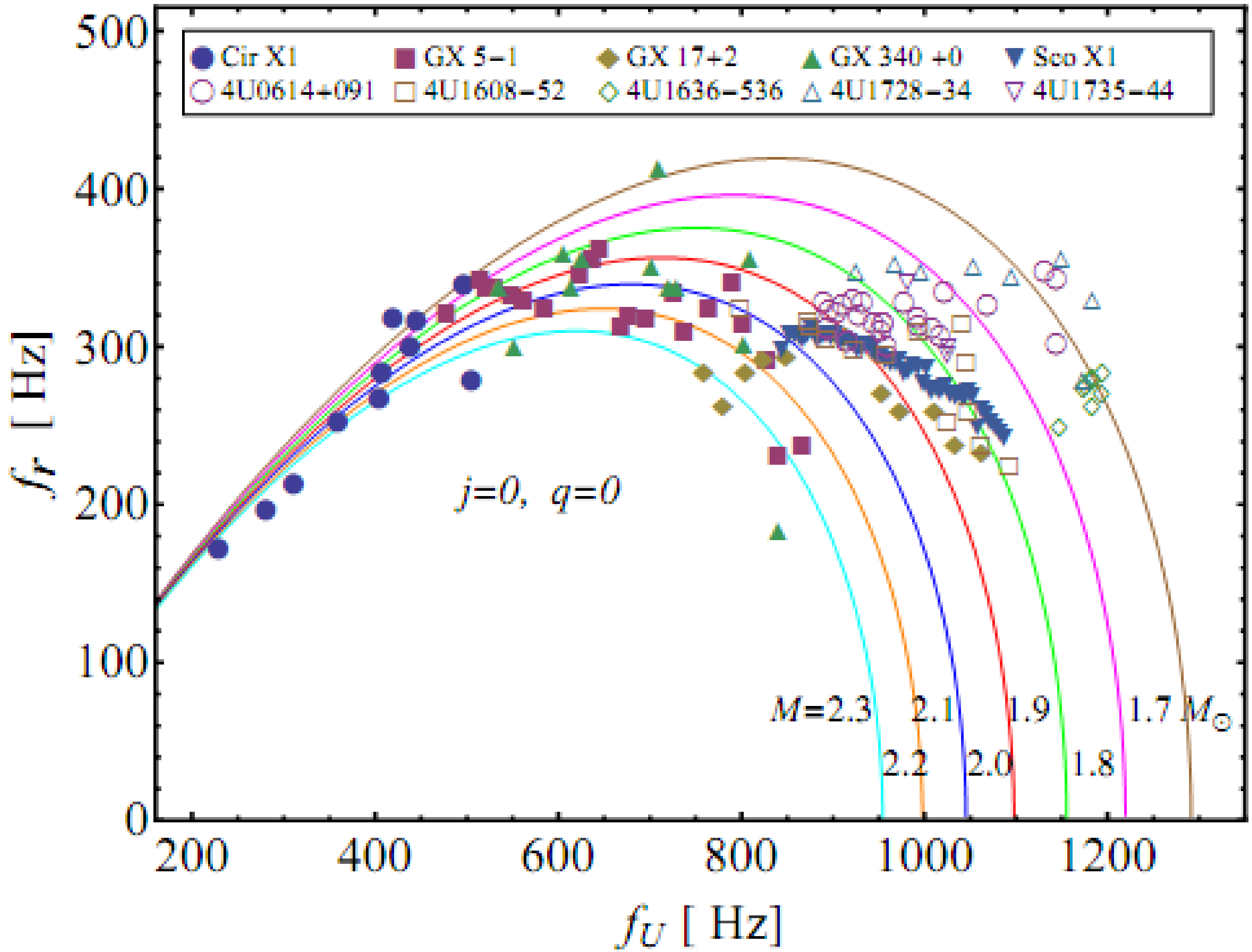

Figure 5 – QPOs from LMXBs

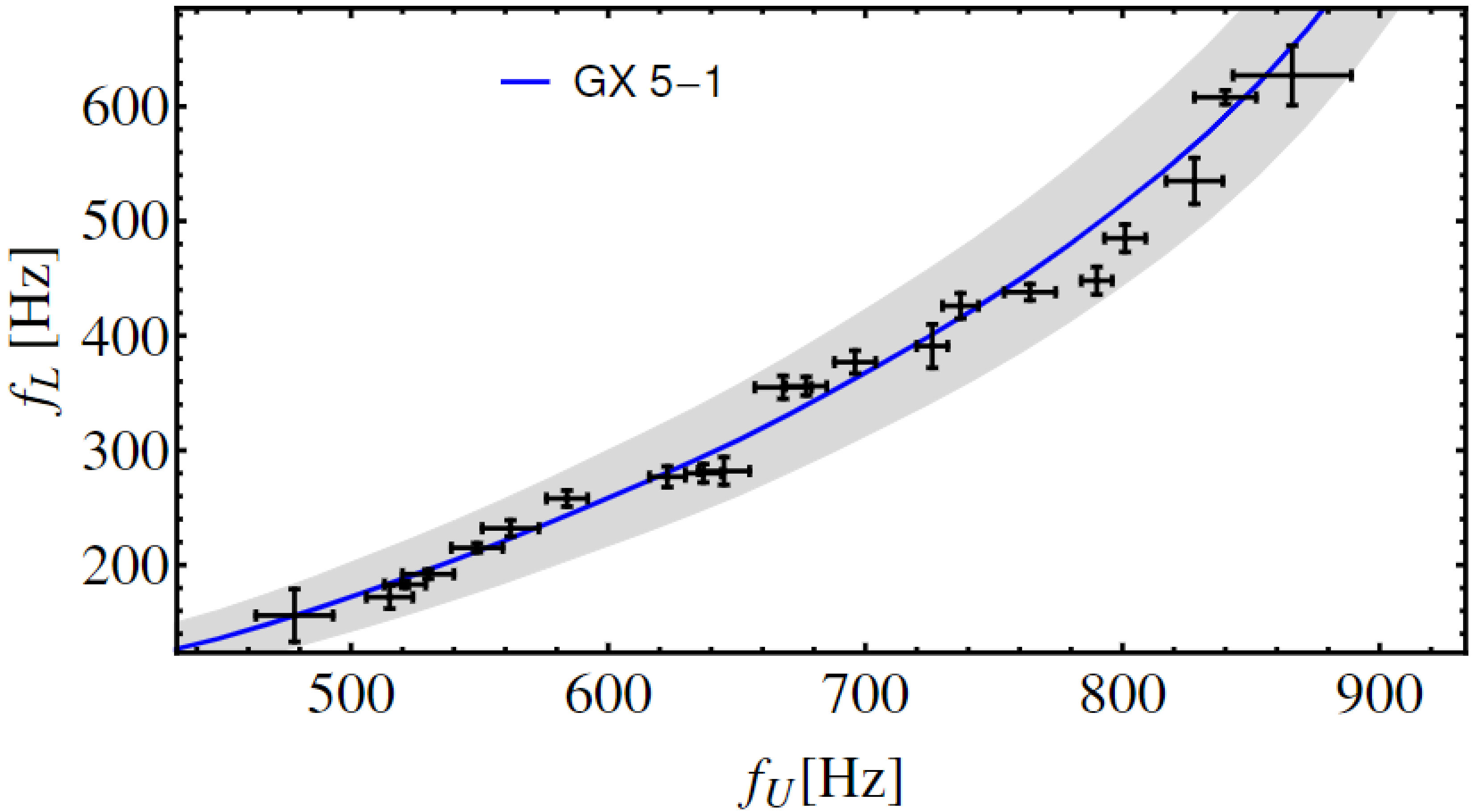

Figure 6 – QPOs from GX 5-1

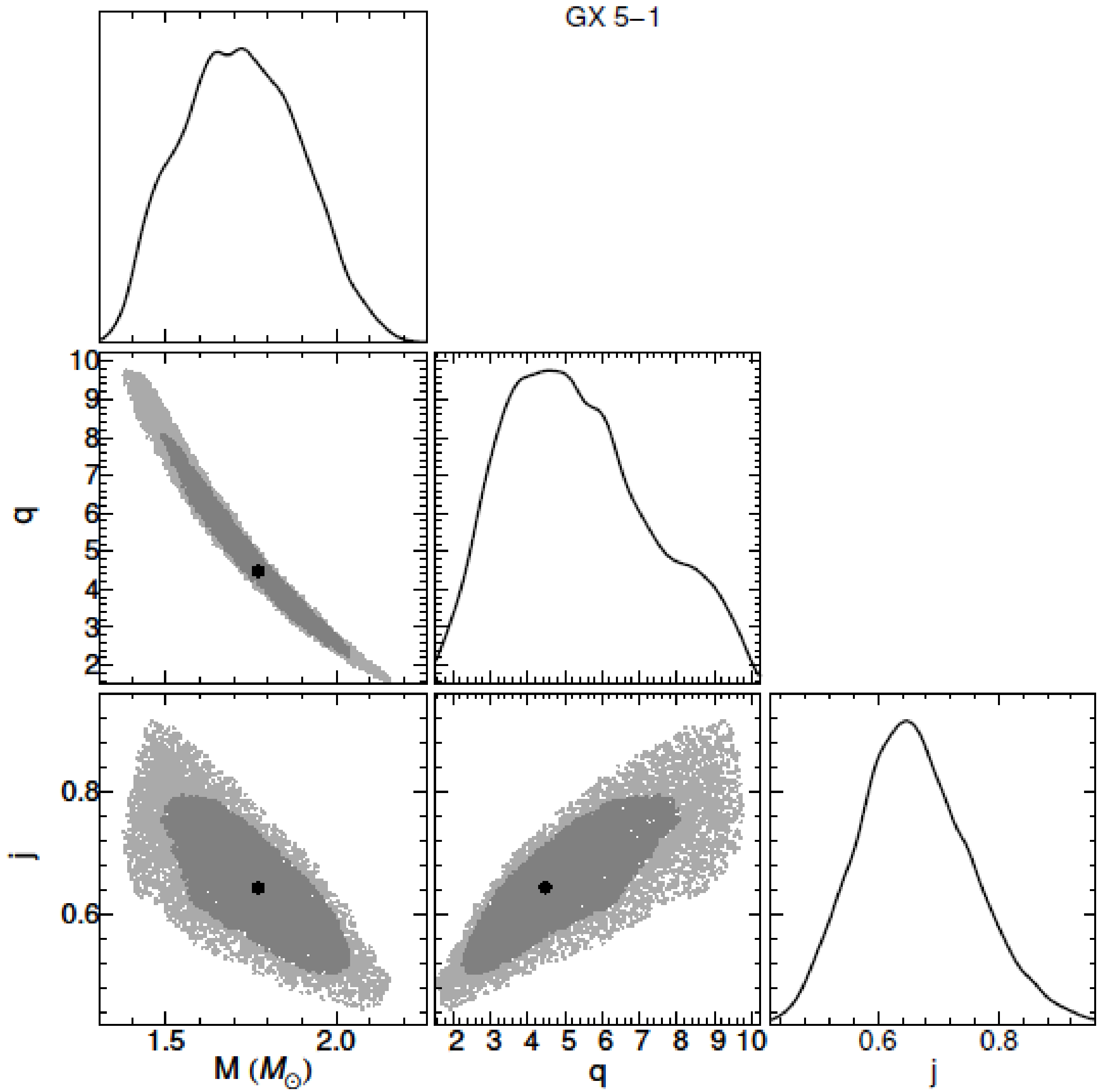

Figure 7 – Contours plots of the best-fit parameters (black dots) and the associated 1–σ (dark gray) and 2–σ (light gray) confidence regions of the source GX 5-1.

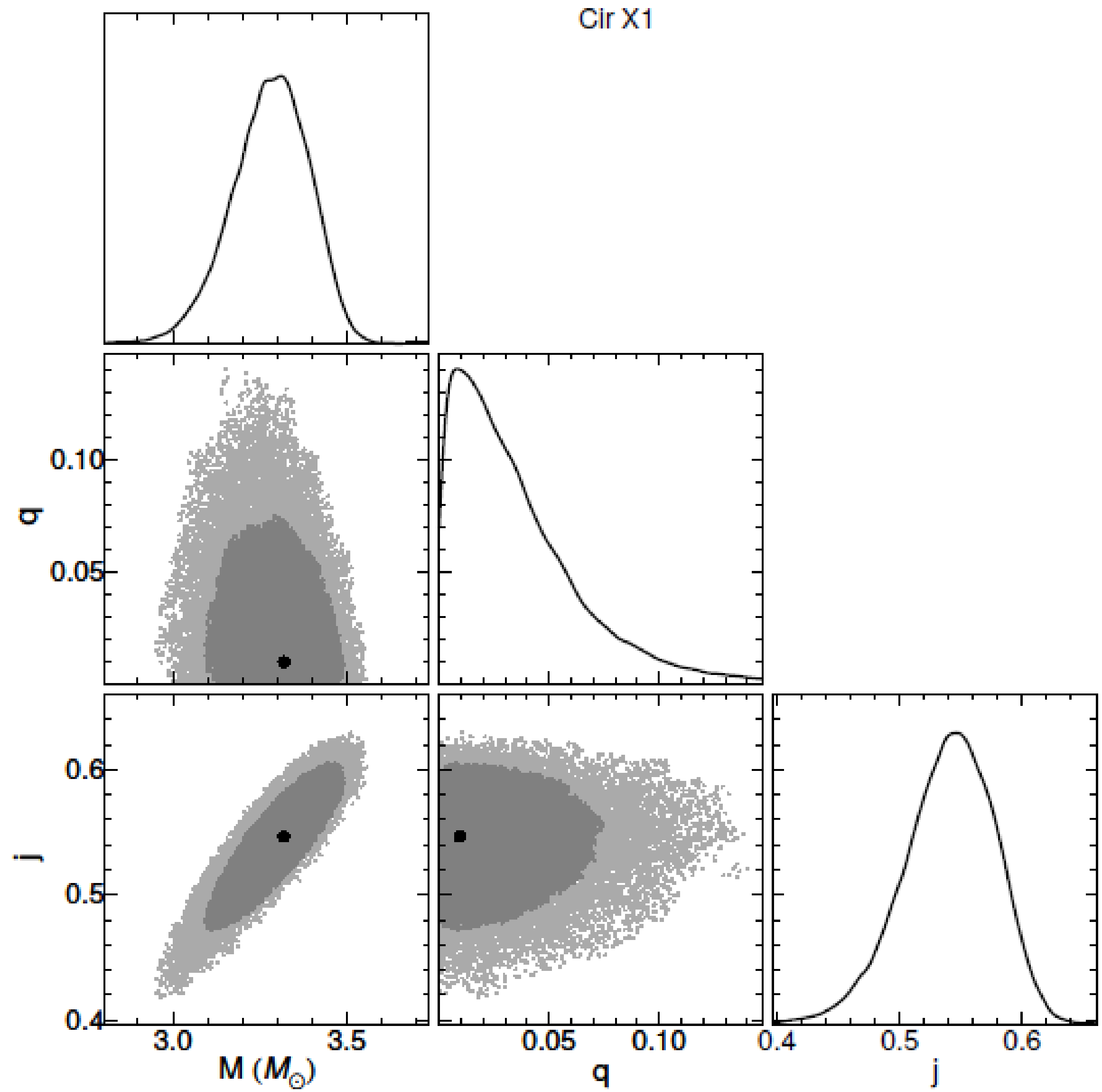

Figure 8 – Contours plots of the best-fit parameters (black dots) and the associated 1–σ (dark gray) and 2–σ (light gray) confidence regions of the source Cir X1.

Source	M $(\mathrm{M}_\odot)$	q	j	$\ln \mathcal{L}_{\max}$	AIC	BIC	ΔAIC	ΔBIC
Cir X1	$2.224^{+0.029}_{-0.029}$	–	–	-125.84	254	254	44	44
	$3.32^{+0.17}_{-0.23}$	$0.010^{+0.065}_{-0.010}$	$0.547^{+0.058}_{-0.075}$	-101.70	210	210	0	0
GX 5-1	$2.161^{+0.010}_{-0.010}$	–	–	-200.33	403	404	184	184
	$1.77^{+0.27}_{-0.28}$	$4.48^{+3.57}_{-2.22}$	$0.64^{+0.15}_{-0.14}$	-105.30	219	220	0	0

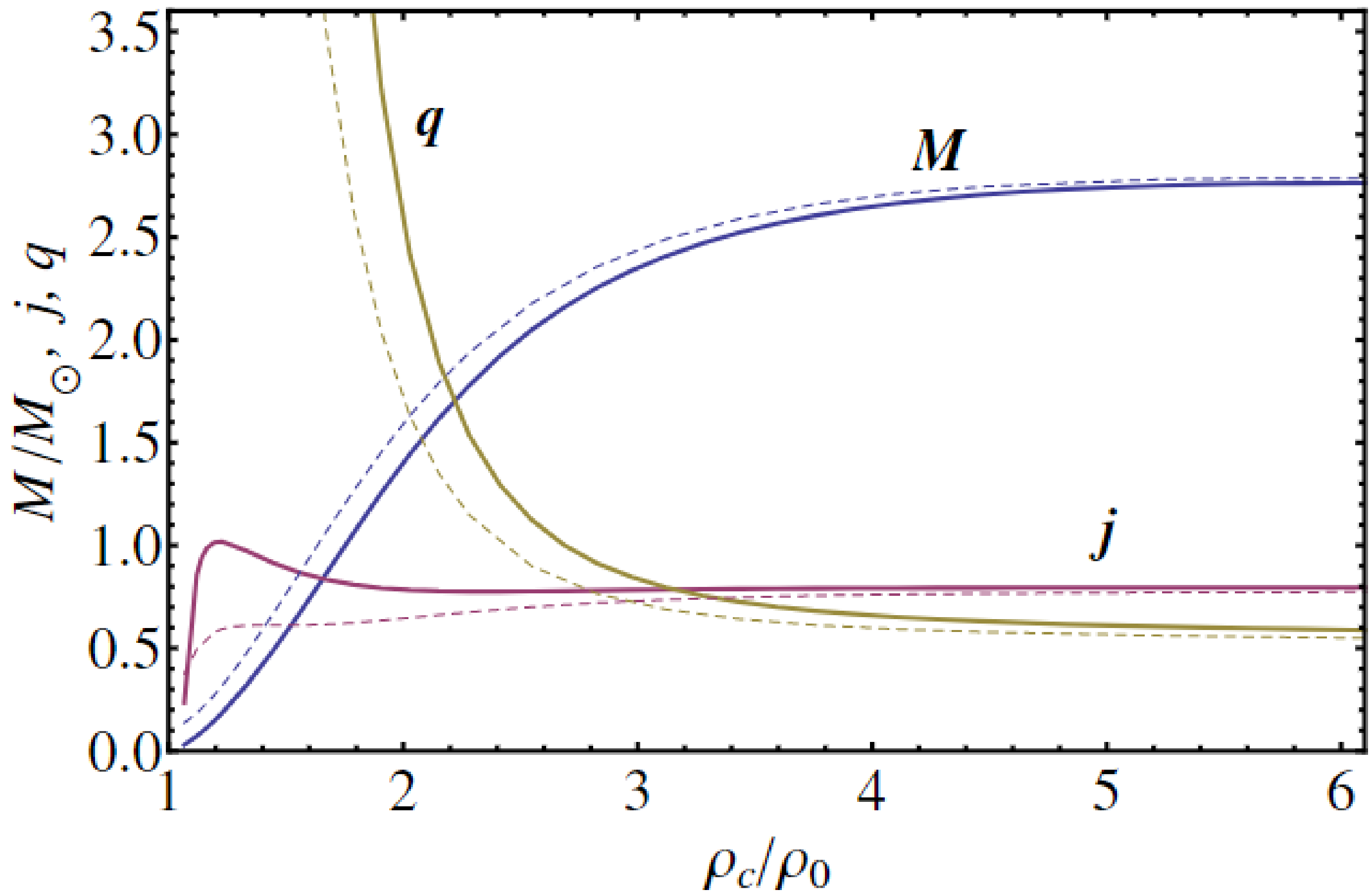

Figure 9 - The mass in solar masses (M/M⊙), the dimensionless angular momentum j and quadrupole moment q as a function of the central density of a maximally rotating neutron star. Solid curves indicate GCN and dashed curves indicate LCN cases.

Conclusion and prospects

- On the basis of the RPM using the QPOs data of GX 5-1 and Cir X1, we inferred the mass, angular momentum and quadrupole moment of the source with error bars (from observation).
- From the neutron star model of Belvedere et. al. (2012, 2014) we derived the rest parameters of the source such as radius, angular velocity (frequency) etc. of the neutron star (from theory).
- Different models for different sources.
- arXiv:2303.03248, arXiv:2212.10186.

Work in progress…

Thank you
for your time and attention!

Type of Radiation	Frequency Range (Hz)	Wavelength Range
Gamma-rays	$10^{20} – 10^{24}$	< 10^{-12} m
X-rays	$10^{17} – 10^{20}$	1 nm – 1 pm
Ultraviolet	$10^{15} – 10^{17}$	400 nm – 1 nm
Visible	$4 \times 10^{14} – 7.5 \times 10^{14}$	750 nm – 400 nm
Near-infrared	$1 \times 10^{14} – 4 \times 10^{14}$	2.5 μm – 750 nm
Infrared	$10^{13} – 10^{14}$	25 μm – 2.5 μm
Microwaves	$3 \times 10^{11} – 10^{13}$	1 mm – 25 μm
Radio waves	< 3×10^{11}	> 1 mm

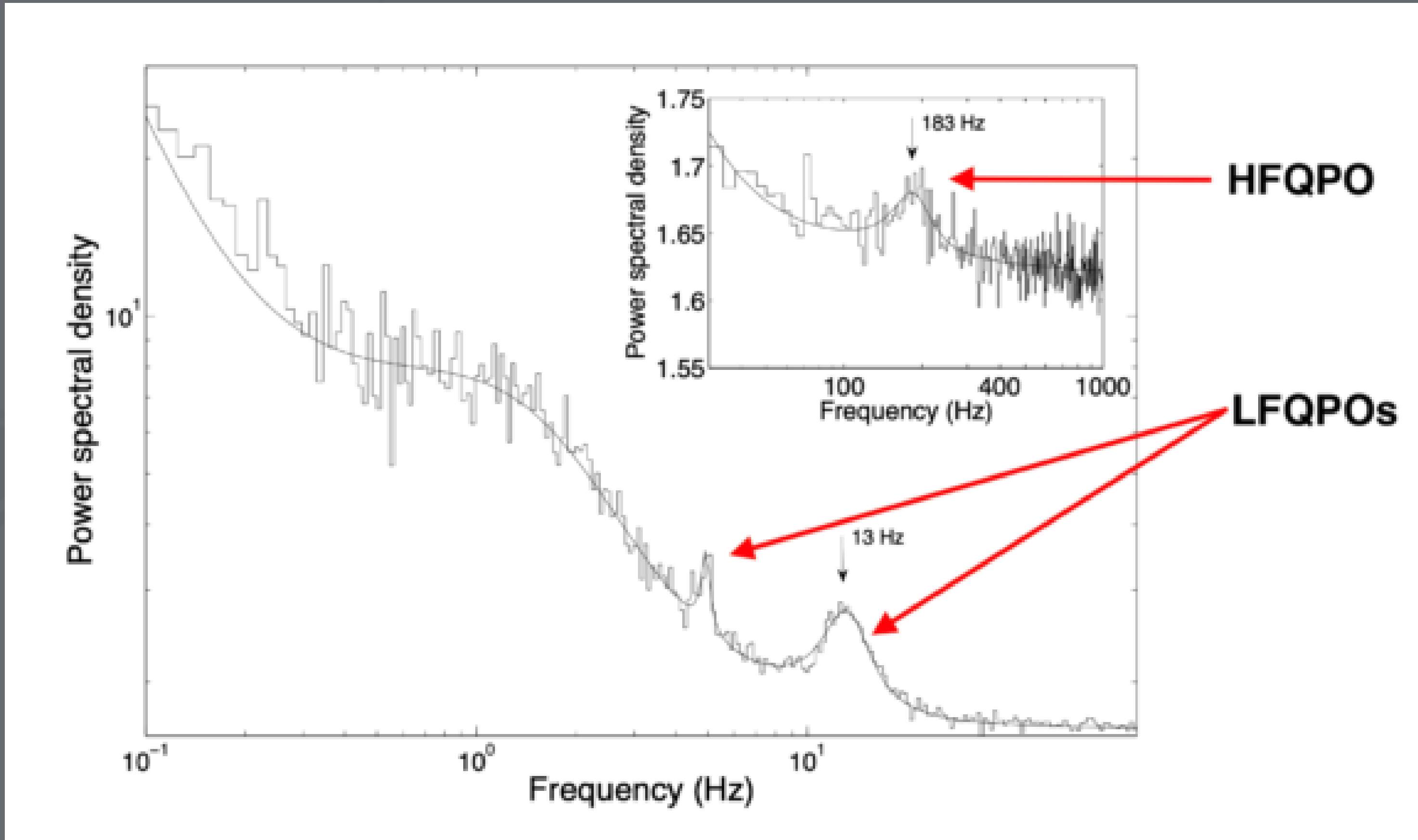

Figure 2. Power density spectrum showing quasi-periodic oscillations (QPOs) in the black hole X-ray binary XTE J1550-564. Credit: Motta et al. 2018.

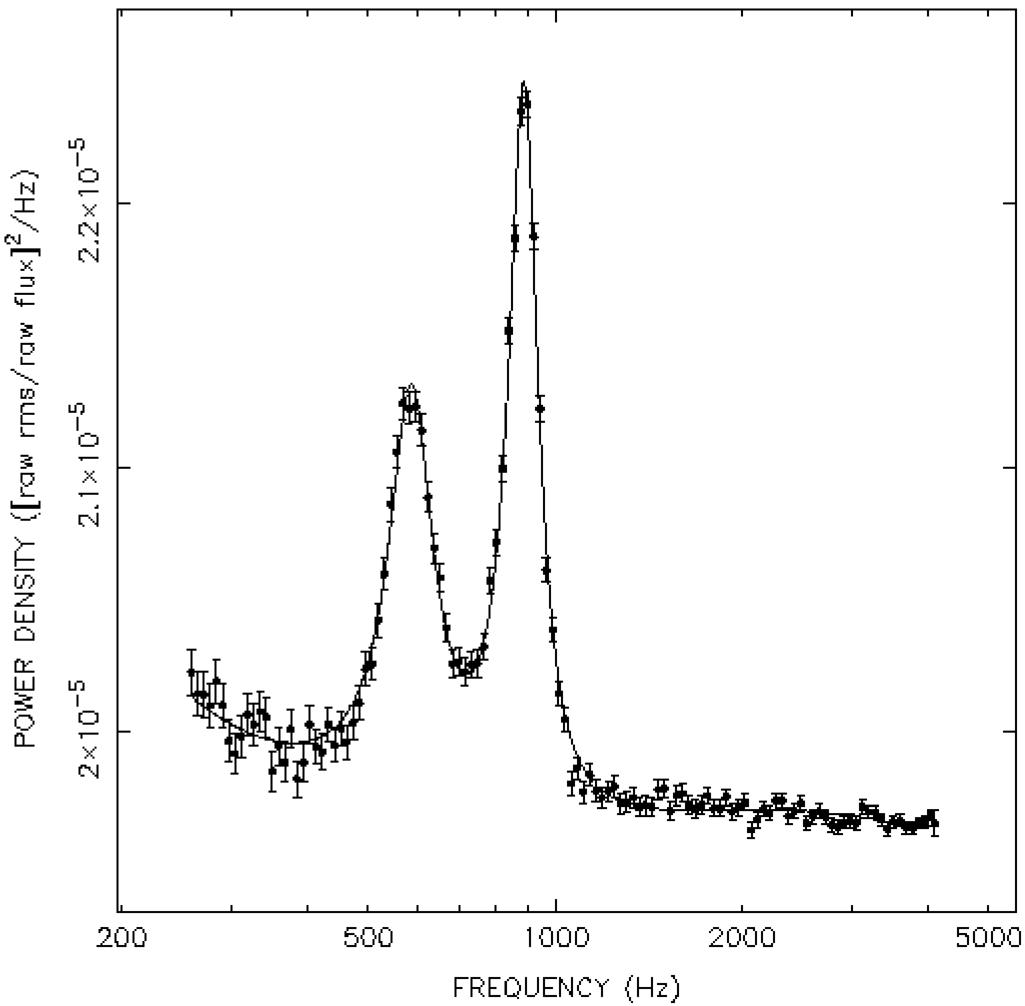

Figure 2: A detailed view of the kilohertz QPO in Sco X-1.